Chapter 5

Diminished liver microperfusion in Fontan patients: a biexponential DWI study

Hildebrand Dijkstra
Djoeke Wolff
Joost P. van Melle
Beatrijs Bartelds
Tineke P. Willems
Matthijs Oudkerk
Hans Hillege
Aad P. van den Berg
Tjark Ebels
Paul E. Sijens

Submitted to NMR in Biomedicine

5.1 Abstract

Background: It has been demonstrated that hepatic apparent diffusion coefficients (ADC) are decreasing in patients with a Fontan circulation. It remains however unclear whether this is a true decrease of molecular diffusion, or rather reflects decreased microperfusion due to decreased portal blood flow.

Purpose: The purpose of this study was therefore to differentiate diffusion and microperfusion using intravoxel incoherent motion (IVIM) modeled diffusion-weighted imaging (DWI) for different liver segments in patients with a Fontan circulation, compare to a control group, and relate with liver function, chronic congestion and hepatic disease.

Materials and Methods: Livers of 59 consecutively included patients with Fontan circulation (29 men; mean-age, 19.1 years) were examined (Oct 2012—Dec 2013) with 1.5T MRI and DWI (b=0, 50, 100, 250, 500, 750, 1500 and 1750 s/mm^2). IVIM (D_{slow}, D_{fast}, f_{fast}) and ADC were calculated for eight liver segments, compared to a control group (19 volunteers; 10 men; mean-age, 32.9 years), and correlated to follow-up duration, clinical variables, and laboratory measurements associated with liver function.

Results: Microperfusion was reduced ($p<0.001$) in Fontan livers compared to controls with −38.1% for D_{fast} and −32.6% for f_{fast}. Molecular diffusion (D_{slow}) was similar between patients and controls, while ADC was significantly lower (−14.3%) in patients ($p<0.001$). ADC decreased significantly with follow-up duration after Fontan operation ($r = -0.657$). D_{slow} showed significant inverse correlations ($r = -0.591$) with follow-up duration whereas D_{fast} and f_{fast} did not.

Conclusions: Decreased hepatic microperfusion was found in Fontan livers compared with controls while molecular diffusion was similar; however, since the Fontan operation molecular diffusion and ADC decreased while microperfusion remained stable.

5.2 Introduction

Diffusion-weighted imaging (DWI) has been successfully applied in the assessment of diffuse liver diseases such as cirrhosis, fibrosis and steatosis (*1–6*). Cirrhotic livers had significantly lower apparent diffusion coefficients (ADC) than normal livers (*2*, *3*, *6*) and negative correlations between fibroses stages and ADC values were demonstrated (*1*, *4*, *5*).

The ADC is obtained by calculating a mono-exponential fit from multiple (al least two) diffusion-weighted images, thereby integrating molecular diffusion and microperfusion effects in one quantitative parameter (*7*, *8*). The concept of the ADC however has been derived from the more complex intravoxel incoherent motion (IVIM) model, which separates molecular diffusion and microperfusion effects by fitting a bi-exponential model to multiple DW images (*8*). It has been suggested that the ADC reduction observed in cirrhotic livers could be linked to decreased microperfusion values and may be related to reduced perfusion (*2*).

A category of patients with altered hepatic perfusion are patients with a Fontan circulation. Fontan et al. described a palliative operation in which the right atrium (and in newer techniques the caval veins) is directly connected to the pulmonary arteries (*9*, *10*). Additional detail about the Fontan operation is provided in the Appendix (5.6).

In the absence of a subpulmonary ventricle, this operation induces increased central venous pressure, decreased preload and increased afterload of the ventricle (*11*). In the Netherlands, yearly around 1200 newborns are born with a congenital heart disease and around 4-5% of these patients have a complex congenital heart disease, known as the univentricular heart, and can be subject for a Fontan operation (*12–14*). Over four decades, the short term survival after the Fontan operation improved significantly, resulting in an increasing cohort of Fontan patients who reach adolescence and adulthood (*15*). Consequently, long-term complications of the Fontan circulation are more commonly seen.

One of the implications of the Fontan circulation is liver disease resulting in fibrosis and cirrhosis (*16–19*). A significant positive correlation has been found between the follow-up duration (number of days since the Fontan operation) and the degree of hepatic fibrosis (*20*). This hepatic damage in the context of a Fontan circulation is presumably caused by the elevated venous pressure and limited cardiac output that causes decreased portal flow (*14*). The hepatic artery compensates the diminished portal flow by increased hepatic arterial flow, which is termed the hepatic arterial buffer response. The distribution of the microperfusion is likely to vary among the different liver seg-

ments due to the alternative distribution of the hepatic flow in Fontan patients.

In a recent report we showed that mean hepatic ADCs are decreased in Fontan patients (*21*). It remained unclear whether this is a true decrease of molecular diffusion, or rather reflects decreased microperfusion due to decreased portal blood flow. Therefore, the aim of our current analysis is to differentiate diffusion and microperfusion using IVIM modeled DWI for different liver segments in patients with a Fontan circulation, compare the results to a control group, and explore the relationship with follow-up duration, liver function, chronic congestion and hepatic disease.

5.3 Materials and methods

5.3.1 Study population

The protocol of this prospective study was approved by the hospital's institutional review board and patients provided informed consent. Between January 2012 and October 2013, consecutive patients with a functionally univentricular heart treated with a Fontan operation (further referred to as Fontan patients) were scheduled for cardiac MRI including diffusion-weighted imaging (DWI) of the liver (*21*). Inclusion criteria were: age 10 years or older. This resulted in 59 patients, 32 children and 27 adults (29 men; mean-age, 19.1 years; age-range, 9.6–44.7 years). All 59 patients have been previously reported (*21*). This prior article dealt with the association between the ADC and functional liver parameters; whereas in this manuscript we apply IVIM modeling to explain the previously observed decreased ADC in Fontan livers by measuring the microperfusion and molecular diffusion in each of eight liver segments.

Clinical variables were available and included body mass index (BMI), cardiac index, ejection fraction, end-diastolic volume (EDV), laboratory measurements (AST, ALT, γ-GT, FactorVIII, AST/ALTratio, bilirubin, albumin, PT), MELDXI (model for end-stage liverdisease excluding INR), Fib-4 (Fibrosis-4 score) and vena cava inferior (VCI) diameter and were obtained using previously described standardized methods (*21*).

In addition, a control group of 19 volunteers was included in this study: 10 men and 9 women (mean-age, 32.9 years; age-range, 20–62 years) (*22*). All volunteers had no relevant medical history.

This study was conducted in accordance with the declaration of Helsinki and was approved by the institutional ethics committee. Informed consent was obtained from all study participants and/or their legally authorized representative.

5.3.2 MR protocols

Diffusion-weighted imaging (DWI) of the liver was acquired by Magnetic Resonance Imaging (MRI), using a commercially available 1.5 T scanner (Magnetom Aera, Siemens Medical Solutions, Erlangen, Germany). A 32 element spine matrix coil in combination with a 4 element body matrix was used as the receiver, and the body coil as transmitter.

The protocol included a routine localizer where after 9 series (b = 0, 50, 100, 250, 500, 750, 1000, 1500 and 1750 s/mm^2) of DWI were acquired using a spin echo based echo-planar imaging (EPI) sequence using the following parameters: TR 5900-9600 ms; TE 90 ms; slice-thickness 5 mm; slice gap 10 mm; FOV 242×300 mm^2; matrix 116×144; bandwidth 1335 Hz/pixel; averages 4 and parallel acquisition technique GRAPPA with acceleration factor 2. PACE respiratory triggering was enabled and spectral adiabatic inversion recovery (SPAIR) was used for fat suppression to avoid artifacts from subcutaneous fat. In total, between 14 and 16 transverse slices were acquired to cover the whole liver within an acquisition time of 2.5 minutes.

5.3.3 DWI analysis

The control group was acquired using 7 b-values (b = 0, 50, 100, 250, 500, 750, 1000 s/mm^2); therefore only these 7 b-values were used in the comparison between Fontan patients and controls, whereas the remaining acquired DWI series (b = 1500 and 1750 s/mm^2) were included in all other analyses.

Drawing of regions-of-interest (ROIs) and the analysis were performed off-line using monoexponential (ADC) and biexponential fitting procedures in a programmable graphical and calculus environment (Matlab, The Mathworks, Natick, MA, USA). Circular ROIs of 21.5 mm^2 were drawn in 8 different segments of the liver (segment II, III, IVa, IVb, V, VI, VII, VIII) according to the Couinaud-Bismuth classification (*23*, *24*). Extra care was taken to avoid major blood vessels in the ROIs.

In the biexponential analyses, the diffusion-weighted signal intensities S were fitted using the parameters prescribed by the IVIM model (*8*, *25*):

$$\frac{S}{S_0} = f_{fast} \cdot \mathrm{e}^{-b \cdot D_{fast}} + f_{slow} \cdot \mathrm{e}^{-b \cdot D_{slow}} \qquad (5.1)$$

where S_o is the maximum signal intensity, D_{fast} is the fast component representing microperfusion, f_{fast} is the fraction of microperfusion, D_{slow} is the slow component repre-

senting molecular diffusion and f_{slow} is the fraction of molecular diffusion ($f_{slow} = 1 - f_{fast}$).

Equation 5.1 was fitted by the Nelder-Mead simplex direct search method with bound constraints, which performs a constrained non-linear minimization of the sum of the squared residuals (*26*, *27*). The initial guess D^0_{slow} was estimated by calculating the slope of the asymptote by monoexponential fitting of the slow signal component between b = 500 and 1000 s/mm², and D_{slow} was bound between 0.2 and $5 \times D^0_{slow} \times 10^{-3}$ mm²/s. The intercept of the asymptote with the y-axis at S_0 resulted in an initial guess f^0_{fast}, and f_{fast} was bound between 0 and 1. The slope of the signal between b = 0 and b = 50 s/mm² was used to guess the initial value of the fast signal component (D^0_{fast}), and D_{fast} was bound between D^0_{slow} (microperfusion can never be slower than molecular diffusion) and 100×10^{-3} mm²/s. The ADC was obtained by using a clinically accepted method: a mono-exponential fit of all b-values was performed.

5.3.4 Statistics

Statistical analyses were performed using SPSS (SPSS 20, Chicago, IL, USA). All data were tested for normality using Shapiro–Wilk tests. IVIM parameters and ADC averaged over all liver segments were compared between Fontan patients and controls by independent samples t-tests. Subsequently, IVIM and ADC were compared per liver segment between Fontan patients and controls by independent samples t-tests. One-way ANOVA tests were used to compare IVIM parameters and ADC between the eight liver segments.

Correlations between DWI (D_{slow}, D_{fast}, f_{fast} and ADC) and clinical laboratory measurements and follow-up duration were calculated using a linear ($Y = a \cdot X + b$) model using Pearson's correlation coefficient for normally distributed variables and Spearman's rank correlation coefficient for non-normally distributed variables.

Normally distributed data were shown as means with standard deviations. Non-normally distributed data were shown as medians with interquartile range. For all statistical tests $p < 0.05$ was considered to indicate a statistically significant difference.

5.4 Results

IVIM-DWI, ADC, AST, ALT, γ-GT, FactorVIII, AST/ALTratio, EDV, EF and Cardiac index were normally distributed ($p \geq 0.071$). Microperfusion parameters (D_{fast} and f_{fast})

averaged over all segments were significantly lower in Fontan patients compared to controls. D_{fast} was 23.2 × 10^{-3} mm^2/s in the liver of Fontan patients, and 37.5 × 10^{-3} mm^2/s in controls ($p<0.001$, −38.1%). F_{fast} was 23.6% in Fontan patients, and 35.0% in controls ($p<0.001$, −32.6%). D_{slow} was similar in patients and controls ranging between 0.95 × 10^{-3} mm^2/s and 1.00 × 10^{-3} mm^2/s ($p = 0.171$). The ADC was significantly lower ($p<0.001$, −14.3%) in Fontan patients (1.08 × 10^{-3} mm^2/s) compared to the controls (1.26 × 10^{-3} mm^2/s).

Also on a segmental level, the microperfusion parameters were significantly decreased for the majority of liver segments of Fontan patients compared to controls (Table 5.1). The molecular diffusion was significantly lower in half of the segments (III, IVb, VI and VII) compared to controls (Table 5.2). The ADC was significantly lower in almost all segments (except segment V).

Concerning the homogeneity of IVIM values among the segments, it was observed that for Fontan patients the microperfusion parameters differed significantly throughout the liver ($p \leq 0.045$). This was also true for the ADC ($p<0.001$). The molecular diffusion however was similar among the segments ($p = 0.208$).

Table 5.1: Microperfusion data (using 7 b-values) per segment. Differences among the segments were tested using one-way ANOVA tests. Differences of DWI data between patients and controls were assessed by independent t-tests. The microperfusion parameters were significantly decreased for the majority of liver segments of Fontan patients compared to controls. Data are mean ± standard deviations. *p-value indicates significant difference

	D_{fast} (×10^{-3} mm^2/s)				F_{fast} (%)			
Seg.	**Controls**	**Patients**	**Δ%**	**p**	**Controls**	**Patients**	**Δ%**	**p**
II	21.5 ± 8.8	27.0 ± 14.1	+25.6	0.051	58.6 ± 12.1	32.6 ± 12.2	-79.8	<0.001*
III	37.7 ± 22.2	24.6 ± 8.9	-53.3	0.021*	37.9 ± 11.0	24.9 ± 9.8	-52.2	<0.001*
IVa	31.2 ± 17.9	23.8 ± 9.5	-30.5	0.095	39.4 ± 16.9	25.1 ± 10.4	-57.0	0.002*
IVb	46.3 ± 16.9	22.9 ± 8.8	-202	<0.001*	35.1 ± 9.5	21.2 ± 7.9	-65.6	<0.001*
V	37.5 ± 13.2	22.2 ± 8.0	-68.9	<0.001*	29.3 ± 6.9	20.4 ± 8.3	-43.6	<0.001*
VI	45.1 ± 23.7	22.4 ± 8.1	-201	0.001*	27.6 ± 9.2	21.3 ± 7.9	-29.6	0.012*
VII	42.9 ± 25.1	21.4 ± 8.9	-200	0.002*	27.1 ± 7.1	21.7 ±6.4	-24.9	0.007*
VIII	37.8 ± 15.2	22.0 ± 8.6	-71.8	<0.001*	24.9 ± 9.7	22.2 ± 7.0	-12.2	0.293
p	0.045*	0.001*			<0.001*	<0.001*		

Table 5.2: Diffusion data (using 7 b-values) per segment. Differences among the segments were tested using one-way ANOVA tests. Differences of DWI data between patients and controls were assessed by independent samples t-tests. The molecular diffusion was significantly lower in half of the segments compared to controls. The ADC of Fontan patients was significantly lower in almost all segments compared to controls (except segment V). Data are mean ± standard deviations. *p-value indicates significant difference

	ADC ($\times 10^{-3}$ mm^2/s)				**D_{slow}** ($\times 10^{-3}$ mm^2/s)			
Seg.	**Controls**	**Patients**	**Δ%**	**p**	**Controls**	**Patients**	**Δ%**	**p**
II	1.42 ± 0.29	1.15 ± 0.28	-23.5	<0.001*	0.79 ± 0.40	0.95 ± 0.36	+16.8	0.123
III	1.38 ± 0.15	1.10 ± 0.15	-25.5	<0.001*	1.12 ± 0.21	0.96 ± 0.19	-16.7	0.009*
IVa	1.40 ± 0.24	1.12 ± 0.16	-25.0	<0.001*	1.05 ± 0.38	0.97 ± 0.23	-8.2	0.422
IVb	1.32 ± 0.15	1.09 ± 0.11	-21.1	<0.001*	1.12 ± 0.14	0.98 ± 0.14	-14.3	0.001*
V	1.09 ± 0.18	1.05 ± 0.12	-3.8	0.391	0.92 ± 0.21	0.96 ± 0.17	+4.2	0.482
VI	1.18 ± 0.08	1.06 ± 0.15	-11.3	<0.001*	1.02 ± 0.09	0.95 ± 0.17	-7.4	0.021*
VII	1.21 ± 0.10	1.06 ± 0.14	-14.2	<0.001*	1.05 ± 0.13	0.93 ± 0.18	-12.9	0.005*
VIII	1.09 ± 0.16	1.00 ± 0.15	-9.0	0.024*	0.94 ± 0.21	0.88 ± 0.20	-6.8	0.213
p	<0.001*	<0.001*			0.001*	0.208		

The DWI data averaged over all segments were correlated to the clinical laboratory measurements (Table 5.3). The median follow-up time was 11.2 years (min: 2.5 years; max: 33.6 years). The ADC showed a significant negative linear relationship with the follow-up duration after Fontan operation with a correlation coefficient r = —0.657 (Fig. 5.1), with the highest correlations found in segments II and VIII (Table 5.4).

Also the molecular diffusion showed a significant negative linear relationship (r = —0.591) with the follow-up duration (Fig. 5.1), with the highest correlations found in segments V and VIII. The microperfusion was stable over time and did not correlate with the follow-up duration (r = —0.158). The fraction of microperfusion on the other hand showed a significant positive linear relationship (r = +0.401) with the follow-up duration (Fig. 5.2(b)), with the highest correlations in segments V and VIII.

The FIB-4 score showed weak though significant relationships, negative with molecular diffusion (r = —0.322) and positive with the fraction of microperfusion (r = +0.324). Some other clinical laboratory parameters also showed significant correlations with IVIM-DWI parameters, most notably gamma GT with ADC and D_{slow} (r = —0.450 and r = —0.424, respectively; Table 5.3).

Table 5.3: Correlations between DWI parameters and clinical variables. †Pearson's correlation coefficient. ‡Spearman's rank correlation coefficient. *p-value indicates significant difference.

	ADC	D_{slow}	D_{fast}	F_{fast}
Laboratory measurements				
AST†	+0.199	+0.275*	+0.250	-0.132
ALT†	-0.173	-0.188	+0.045	+0.218
gamma GT†	-0.450*	-0.424*	-0.047	+0.199
Bilirubin‡	-0.258	-0.275	+0.198	+0.301*
Albumin‡	+0.127	+0.100	+0.238	+0.110
PT‡	-0.143	-0.180	-0.321*	-0.033
Factor VIII†	+0.046	-0.003	-0.058	+0.005
Liver disease scores				
MELDXI‡	-0.259	-0.271	+0.266	+0.402*
AST-ALT ratio†	+0.330*	+0.405*	+0.203	-0.317*
Fib-4‡	-0.344*	-0.322*	-0.020	+0.324*
Cardiac function				
EDV†	+0.153	+0.093	+0.031	+0.131
EF†	+0.043	+0.076	+0.070	-0.106
Cardiac-index†	+0.270*	+0.266*	+0.220	+0.005
VCI diameter‡	-0.222	-0.211	0.034	0.180
Follow-up duration†	-0.657*	-0.591*	-0.158	+0.401*

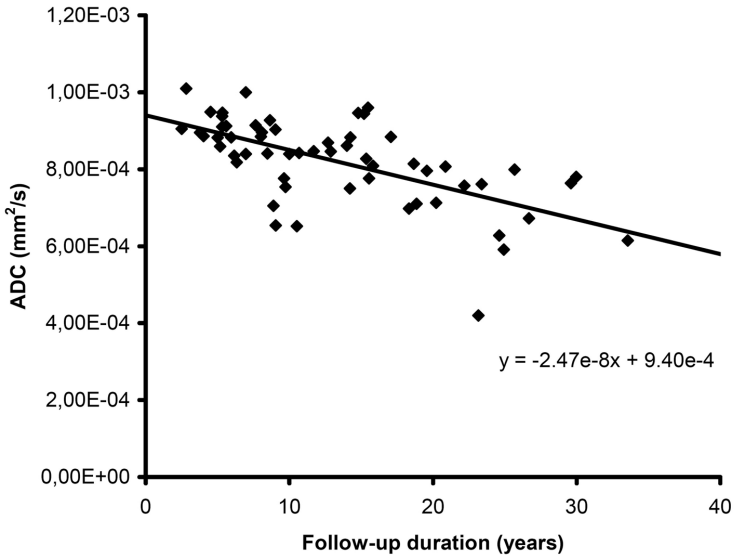

Figure 5.1: Correlation between follow-up duration and apparent diffusion coefficient (ADC). The mean hepatic ADC for each patient (n = 59) is plotted against the number of years since the Fontan operation (follow-up duration). The ADC showed a significant negative linear relationship with the follow-up duration (r = —0.657).

Table 5.4: Follow-up duration and DWI parameters correlated per segment. Data are Spearman's rank correlation coefficients. *p-value indicates significant difference.

Segment	ADC	D_{slow}	D_{fast}	F_{fast}
II	-0.632*	-0.307*	+0.002	-0.167
III	-0.447*	-0.397*	+0.067	+0.239
IVa	-0.555*	-0.453*	-0.216	+0.212
IVb	-0.367*	-0.258	+0.013	+0.221
V	-0.562*	-0.556*	-0.120	+0.440*
VI	-0.494*	-0.488*	-0.123	+0.269*
VII	-0.328*	-0.367*	-0.207	+0.203
VIII	-0.612*	-0.567*	-0.154	+0.371*

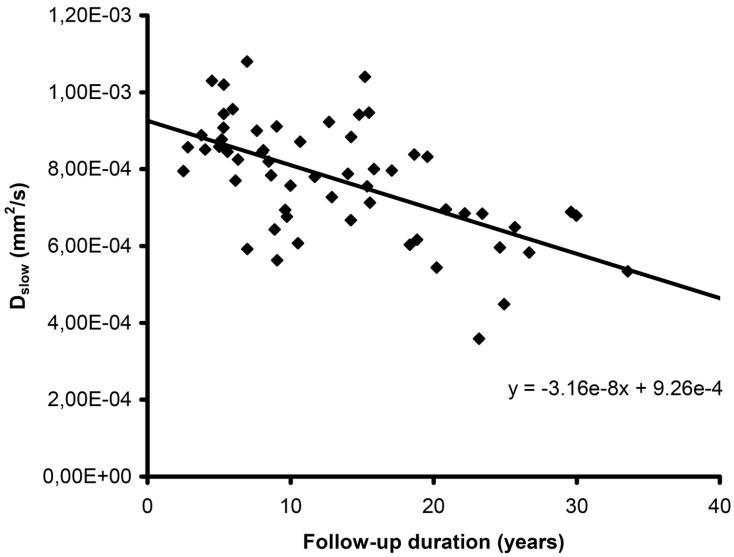

((a)) Follow-up duration vs. molecular diffusion (D_{slow}).

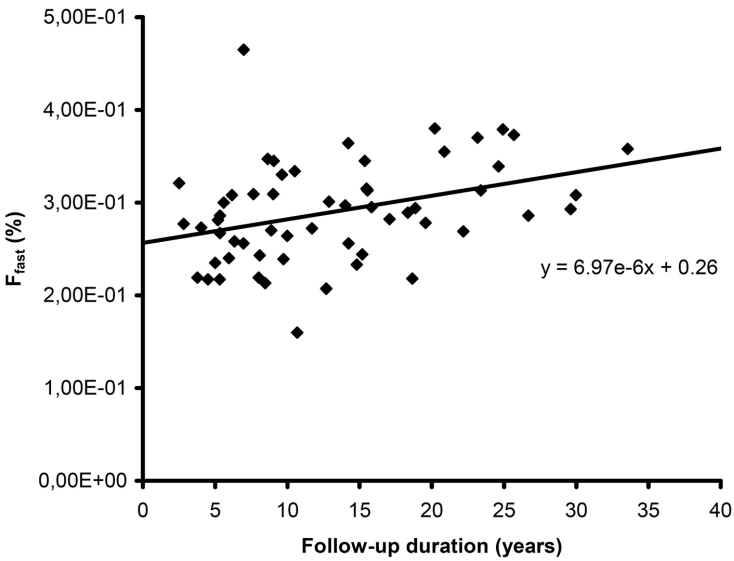

((b)) Follow-up duration vs. fraction of microperfusion (f_{fast}).

Figure 5.2: Correlation between follow-up duration and molecular diffusion (top) and microperfusion (bottom). The mean is plotted for each patient (n = 59) against the number of years since the Fontan operation (follow-up duration). D_{slow} showed a significant negative linear relationship (r = —0.591) with the follow-up duration, whereas the f_{fast} showed a a significant positive linear relationship (r = +0.401)

5.5 Discussion

This study demonstrates that decreased hepatic ADC measurements of Fontan patients can be explained by significantly lower microperfusion in the Fontan liver rather than by decreased diffusion. It was observed that the molecular diffusion (D_{slow}) was similar between Fontan patients and controls, while the microperfusion parameters (D_{fast} and f_{fast}) and ADC were significantly lower in the Fontan liver. A previously formulated hypothesis relating hypoperfusion of the liver to the reduced ADC in Fontan patients is thus substantiated (*21*).

However, the currently and previously (*21*) reported strong negative dependency of the hepatic ADC on the follow-up duration after the Fontan operation, reflects changes of the molecular diffusion with time rather than changes of the microperfusion with time. This potentially indicates that in the Fontan patient's follow-up true cellular changes leading to fibrosis and cirrhosis dominate over changes in microperfusion.

The evidence in the current study that hypoperfusion of the liver in Fontan patients causes the reduced ADC values as compared with controls, confirms the high degree of sensitivity to microperfusion of the mono-exponential model which was already shown decades ago by Le Bihan et al. in DWI of the brain (*8*). When the DWI sequence contains b-values in the microperfusion range ($b \leq 100$ s/mm^2), and the microperfusion is diminished, the ADC measurements will decrease (*22*). With a bi-exponential IVIM model, the cellular diffusion component can be distinguished from the microperfusion component, in order to improve our understanding of the underlying pathophysiology of liver disease in the Fontan circulation, and to provide important additional information on the degree of congestion and liver fibrosis and cirrhosis in clinical practice.

It was observed that the ADC values and molecular diffusion decreased with the follow-up duration after Fontan operation, whereas the microperfusion was stable over time. In other words, structural liver disease (i.e. liver fibrosis or cirrhosis) seems not present at first but develops progressively in time after Fontan operation whereas the hepatic congestion is chronically present and stable over time.

All patients had some derangement of laboratory liver measurements; potentially laboratory disturbance is not only associated with advanced liver disease, but also influenced by chronic liver damage, due to congestion and hypoperfusion. Increased gamma GT, a sign of congestive hepatopathy, was related to D_{slow} and unrelated to the microperfusion. This suggests that D_{slow} is potentially related to liver fibrosis and cirrhosis, and suggests that in the liver these processes might develop faster in context of more liver congestion (as in the first case report by Lemmer in 1983) (*28*).

Previous histological studies have demonstrated, on a microscopic level, that in patients with chronic hepatic congestion, the poorly arterially supplied hepatocytes in the centrilobular zone show atrophy (*29*, *30*). In patients with a Fontan circulation, atrophy of centrilobular hepatocytes seems related to the degree of right sided pressure and to the time after Fontan operation (*20*, *30*). Likewise, on a macroscopic level, the arterial blood supply is not homogenously distributed over the various liver segments. It has been reported that the ratio of the arterial liver perfusion (ALP) and portal venous perfusion (PVP) varies and is the lowest in segments V to VIII and highest in segments I to IV (*31*, *32*). When the ALP over-compensates the PVP in Fontan patients, it is expected that the microperfusion increases in segments I to IV, and diminishes in segments V to VIII. This is confirmed by our data. This suggests that, in a Fontan circulation, the development of liver fibrosis or cirrhosis varies between the different liver segments, depending on the degree of arterial blood supply.

Altogether, this study demonstrated that the degree of congestion is generally stable with time after Fontan operation, whereas liver fibrosis/-cirrhosis develops progressively. With the bi-exponential model, the DWI-MR technique provides the opportunity to distinguish between these two components. For clinical practice, this provides a major advantage compared to the other non-invasive alternatives for liver biopsy. Potentially, a decrease in the microperfusion component could indicate an adverse change in the Fontan circulation, for instance more congestion due to a conduit stenosis or pulmonary vascular remodeling. With a routine follow-up of the cellular diffusion, the development of liver fibrosis/-cirrhosis can be safely monitored.

We suggest further research to investigate changes in microperfusion and cellular diffusion longitudinally, and want to highlight that, with progressive liver disease being apparently inherent to the Fontan circulation, steps have to be taken concerning potential treatment options for liver disease in Fontan patients. Therefore, future studies should focus on reversibility of this liver disease, and the effects and timing of potential treatment options, including heart transplantation, Fontan conversion or a late Fontan takedown.

5.5.1 Limitations

Liver damage in the Fontan circulation presents with disturbed transaminases, coagulation disorders, and can eventually lead to liver fibrosis-, cirrhosis and even hepatocellular carcinoma (*33–35*). It was assumed that the severity of fibrosis increases with

the follow-up duration after Fontan operation. The stage of liver fibrosis or cirrhosis was however not confirmed by liver biopsy, thereby limiting the study.

Although the segmental differences in microperfusion strongly point to the reported variation in the ALP and PVP in Fontan patients, this might also be related to cardiac pulsation artifacts in DWI which are known to result in deviating values between right and left liver lobe. The increase in the ADC in the left lobe is usually explained from the increased cardiac motion in the left lobe (*36–40*). However, it was also demonstrated that the increased ADC in the left lobe may be caused by extensive microperfusion contamination of the ADC and this does not affect the molecular diffusion obtained by IVIM (*22*). This effect of microperfusion contamination in the left lobe is also supported by the observed tendency of increased D_{fast} in segment II against the trend in all other segments.

5.5.2 Conclusions

Decreased hepatic microperfusion was found in Fontan livers compared with controls while the molecular diffusion was similar. The molecular diffusion and ADC decreased since the Fontan operation while the microperfusion remained stable. The current study is the first to show with IVIM-DWI that, in a Fontan circulation, the development of liver fibrosis or cirrhosis varies between the different liver segments, depending on the degree of arterial blood supply.

5.6 Appendix: The Fontan operation

The Fontan operation is currently the treatment-of-choice for patients who are born with a univentricular heart which is not suitable for a biventricular repair (*9*, *10*). With the Fontan operation, the right atrium or both caval veins are surgically connected to the pulmonary artery, thereby bypassing the subpulmonary ventricle. This means that the systemic venous return flows passively through the pulmonary vascular bed, without the aid of a pumping ventricle. As a consequence, Fontan patients suffer from chronically elevated systemic venous pressure and decreased cardiac output due to decreased ventricular preload and increased ventricular afterload.

Over four decades, the short term survival after the Fontan operation improved significantly (*15*). However, patients who underwent a Fontan operation are prone to develop several complications on the long-term. The liver is one of the organs that suffer

from the unphysiologic circumstances. Both the increased systemic venous pressure and the decreased cardiac output are thought to be underlying causes of the progressive liver damage in the Fontan circulation.

The liver damage in the Fontan circulation was first recognized in a 15-year-old girl with severe systemic hypertension due to a conduit stenosis (*28*). Nowadays, more evidence is emerging that liver damage is not restricted to single patients with adverse hemodynamic complications, but is inherently related to the un-physiological circumstances of the Fontan circulation (*21*).

Liver damage in the Fontan circulation presents with disturbed transaminases, coagulation disorders, and can eventually lead to liver fibrosis-, cirrhosis and even hepatocellular carcinoma (*33–35*). Because a liver biopsy (which is considered the golden standard) is hazardous in Fontan patients, the search for alternative measures to assess liver fibrosis and cirrhosis is ongoing.

5.7 References

(*1*) Bakan, A. A., Inci, E., Bakan, S., Gokturk, S., and Cimilli, T. (2012). Utility of diffusion-weighted imaging in the evaluation of liver fibrosis. *European radiology 22*, 682–687.

(*2*) Luciani, A. et al. (2008). Liver cirrhosis: intravoxel incoherent motion MR imaging–pilot study. *Radiology 249*, 891–899.

(*3*) Patel, J., Sigmund, E. E., Rusinek, H., Oei, M., Babb, J. S., and Taouli, B. (2010). Diagnosis of cirrhosis with intravoxel incoherent motion diffusion MRI and dynamic contrast-enhanced MRI alone and in combination: preliminary experience. *Journal of magnetic resonance imaging : JMRI 31*, 589–600.

(*4*) Lewin, M. et al. (2007). Diffusion-weighted magnetic resonance imaging for the assessment of fibrosis in chronic hepatitis C. *Hepatology (Baltimore, Md.) 46*, 658–665.

(*5*) Wang, Y. et al. (2011). Assessment of chronic hepatitis and fibrosis: comparison of MR elastography and diffusion-weighted imaging. *AJR.American journal of roentgenology 196*, 553–561.

(*6*) Amano, Y., Kumazaki, T., and Ishihara, M. (1998). Single-shot diffusion-weighted echo-planar imaging of normal and cirrhotic livers using a phased-array multicoil. *Acta Radiologica (Stockholm, Sweden : 1987) 39*, 440–442.

(*7*) Namimoto, T., Yamashita, Y., Sumi, S., Tang, Y., and Takahashi, M. (1997). Focal liver masses: characterization with diffusion-weighted echo-planar MR imaging. *Radiology 204*, 739–744.

(*8*) Bihan, D. L., Breton, E., Lallemand, D., Aubin, M. L., Vignaud, J., and Laval-Jeantet, M. (1988). Separation of diffusion and perfusion in intravoxel incoherent motion MR imaging. *Radiology 168*, 497–505.

(*9*) Fontan, F., and Baudet, E. (1971). Surgical repair of tricuspid atresia. *Thorax 26*, 240–248.

(*10*) Kreutzer, G., Galindez, E., Bono, H., Palma, C. D., and Laura, J. P. (1973). An operation for the correction of tricuspid atresia. *The Journal of thoracic and cardiovascular surgery 66*, 613–621.

(*11*) Fredenburg, T. B., Johnson, T. R., and Cohen, M. D. (2011). The Fontan procedure: anatomy, complications, and manifestations of failure. *Radiographics : a review publication of the Radiological Society of North America, Inc 31*, 453–463.

(*12*) Cornel, M. Aangeboren afwijkingen van het hartvaatstelsel: prevalentie en sterfte naar leeftijd en geslacht. In: Volksgezondheid Toekomst Verkenning, Nationaal Kompas Volksgezondheid. Bilthoven: RIVM, http://www.nationaalkompas.nl/gezondheid-en-ziekte/ziekten-en-aandoeningen/aangeboren-afwijkingen/hartvaatstelsel/hoe-vaak-komen-aangeboren-afwijkingen-van-het-hartvaatstelsel-voor/., 2010.

(*13*) Hoffman, J. I., and Kaplan, S. (2002). The incidence of congenital heart disease. *Journal of the American College of Cardiology 39*, 1890–1900.

(*14*) Rychik, J. et al. (2012). The precarious state of the liver after a Fontan operation: summary of a multidisciplinary symposium. *Pediatric cardiology 33*, 1001–1012.

(*15*) Wolff, D., van Melle, J. P., Ebels, T., Hillege, H., van Slooten, Y. J., and Berger, R. M. (2014). Trends in mortality (1975-2011) after one- and two-stage Fontan surgery, including bidirectional Glenn through Fontan completion. *European journal of cardio-thoracic surgery : official journal of the European Association for Cardio-thoracic Surgery 45*, 602–609.

(*16*) Greenway, S. C. et al. (2015). Fontan-associated liver disease: Implications for heart transplantation. *The Journal of heart and lung transplantation : the official publication of the International Society for Heart Transplantation*.

(*17*) Pundi, K. et al. (2015). Liver Disease in Patients After the Fontan Operation. *The American Journal of Cardiology*.

(*18*) Ozkurt, H., Keskiner, F., Karatag, O., Alkim, C., Erturk, S. M., and Basak, M. (2014). Diffusion Weighted MRI for Hepatic Fibrosis: Impact of b-Value. *Iranian journal of radiology : a quarterly journal published by the Iranian Radiological Society 11*, e3555.

(*19*) Sandrasegaran, K. et al. (2009). Value of diffusion-weighted MRI for assessing liver fibrosis and cirrhosis. *AJR.American journal of roentgenology 193*, 1556–1560.

(*20*) Kiesewetter, C. H. et al. (2007). Hepatic changes in the failing Fontan circulation. *Heart (British Cardiac Society) 93*, 579–584.

(*21*) Wolff, D. et al. (2016). The Fontan circulation and the liver: A magnetic resonance diffusion-weighted imaging study. *International journal of cardiology 202*, 595–600.

(*22*) Dijkstra, H., Baron, P., Kappert, P., Oudkerk, M., and Sijens, P. E. (2012). Effects of microperfusion in hepatic diffusion weighted imaging. *European radiology 22*, 891–899.

(*23*) Couinaud, C., *Le foie: etudes anatomiques et chirurgicales*; Masson: Paris, 1957.

(*24*) Bismuth, H. (1982). Surgical anatomy and anatomical surgery of the liver. *World journal of surgery 6*, 3–9.

(*25*) Bihan, D. L., Turner, R., Moonen, C. T., and Pekar, J. (1991). Imaging of diffusion and microcirculation with gradient sensitization: design, strategy, and significance. *Journal of magnetic resonance imaging : JMRI 1*, 7–28.

(*26*) Muller, M. F., Prasad, P., Siewert, B., Nissenbaum, M. A., Raptopoulos, V., and Edelman, R. R. (1994). Abdominal diffusion mapping with use of a whole-body echo-planar system. *Radiology 190*, 475–478.

(*27*) Turner, R., Bihan, D. L., Maier, J., Vavrek, R., Hedges, L. K., and Pekar, J. (1990). Echo-planar imaging of intravoxel incoherent motion. *Radiology 177*, 407–414.

(*28*) Lemmer, J. H., Coran, A. G., Behrendt, D. M., Heidelberger, K. P., and Stern, A. M. (1983). Liver fibrosis (cardiac cirrhosis) five years after modified Fontan operation for tricuspid atresia. *The Journal of thoracic and cardiovascular surgery 86*, 757–760.

(*29*) Safran, A. P., and Schaffner, F. (1967). Chronic passive congestion of the liver in man. Electron microscopic study of cell atrophy and intralobular fibrosis. *The American journal of pathology 50*, 447–463.

(*30*) Ghaferi, A. A., and Hutchins, G. M. (2005). Progression of liver pathology in patients undergoing the Fontan procedure: Chronic passive congestion, cardiac cirrhosis, hepatic adenoma, and hepatocellular carcinoma. *The Journal of thoracic and cardiovascular surgery 129*, 1348–1352.

(*31*) Kanda, T. et al. (2012). Perfusion measurement of the whole upper abdomen of patients with and without liver diseases: initial experience with 320-detector row CT. *European Journal of Radiology 81*, 2470–2475.

(*32*) Wang, X. et al. (2013). Quantitative hepatic CT perfusion measurement: comparison of Couinaud's hepatic segments with dual-source 128-slice CT. *European Journal of Radiology 82*, 220–226.

(*33*) Johnson, J. A. et al. (2013). Identifying predictors of hepatic disease in patients after the Fontan operation: a postmortem analysis. *The Journal of thoracic and cardiovascular surgery 146*, 140–145.

(*34*) Asrani, S. K. et al. (2012). Congenital heart disease and the liver. *Hepatology (Baltimore, Md.) 56*, 1160–1169.

(*35*) Asrani, S. K., Warnes, C. A., and Kamath, P. S. (2013). Hepatocellular carcinoma after the Fontan procedure. *The New England journal of medicine 368*, 1756–1757.

(*36*) Boulanger, Y. et al. (2003). Diffusion-weighted MR imaging of the liver of hepatitis C patients. *NMR in biomedicine 16*, 132–136.

(*37*) Nasu, K., Kuroki, Y., Sekiguchi, R., Kazama, T., and Nakajima, H. (2006). Measurement of the apparent diffusion coefficient in the liver: is it a reliable index for hepatic disease diagnosis? *Radiation Medicine 24*, 438–444.

(*38*) Koh, D. M. et al. (2006). Colorectal hepatic metastases: quantitative measurements using single-shot echo-planar diffusion-weighted MR imaging. *European radiology 16*, 1898–1905.

(*39*) Kandpal, H., Sharma, R., Madhusudhan, K. S., and Kapoor, K. S. (2009). Respiratory-triggered versus breath-hold diffusion-weighted MRI of liver lesions: comparison of image quality and apparent diffusion coefficient values. *AJR.American journal of roentgenology 192*, 915–922.

(*40*) Kwee, T. C. et al. (2009). Influence of cardiac motion on diffusion-weighted magnetic resonance imaging of the liver. *Magma (New York, N.Y.) 22*, 319–325.

Part III

Breast